
Diffusion Probabilistic Models for Super Resolution Microscopy

Anonymous Author(s)

Affiliation

Address

email

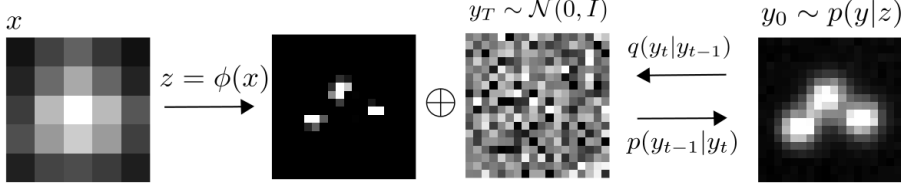
Abstract

1 Single-molecule localization microscopy (SMLM) techniques are a mainstay of
2 fluorescence microscopy and can be used to produce a pointillist representation
3 of living cells at diffraction-unlimited precision. Classical SMLM approaches
4 leverage the deactivation of fluorescent tags, followed by spontaneous or pho-
5 toinduced reactivation, which can be used to estimate of the density of a tagged
6 biomolecule in cellular compartments. Standard SMLM localization algorithms
7 based on maximum likelihood estimators or least squares optimization require
8 tight control of activation and reactivation to maintain sparse emitters, present-
9 ing a tradeoff between imaging speed and labeling density. Deep models have
10 generalized SMLM to densely labeled structures, yet uncertainty quantification
11 is still lacking. Recently, denoising diffusion probabilistic models (DDPMs) have
12 been adapted conditional super resolution tasks, demonstrating promising results
13 in detail reconstruction, while directly providing uncertainties in model predictions.
14 Here, we adapt DDPM to the task of single molecule localization, and demonstrate
15 that DDPM approaches the Cramer-Rao lower bound on localization uncertainty
16 over a wide range of experimental conditions.

17 1 Introduction

18 Single molecule localization microscopy (SMLM) relies on the temporal resolution of fluorophores
19 whose spatially overlapping point spread functions would otherwise render them unresolvable at the
20 detector. Common strategies for the temporal separation of molecules involve transient intramolecular
21 rearrangements to switch from dark to fluorescent states or the exploitation of non-emitting molecular
22 radicals. Estimation of molecular coordinates in SMLM is achieved by modeling the optical impulse
23 response of the imaging system. However, dense localization suffers from the curse of dimensionality
24 - the parameter space volume grows exponentially with the number of molecules, which is often
25 unknown a priori. Exploration of this high dimensional parameter space in dense SMLM is often
26 intractable.

27 Previous approaches to this issue has been to predict super-resolution images from a sparse set of
28 localizations with conditional generative adversarial networks (Ouyang 2018) or direct prediction of
29 coordinates using deep neural networks (Nehme 2020; Speiser 2021). However, diffusion models are
30 an appealing alternative because they infer a distribution of deconvolved images that are compatible
31 with an observation. Although conditional VAEs and conditional GANs can provide a distribution of
32 deconvolved images, both are known to suffer from mode collapse and produce insufficient diversity
33 in their outputs. Diffusion models are a recently developed alternative to VAEs and GANs that excel
34 at producing diverse samples and have been successfully applied to solve inverse problems. Here,
35 we present a novel diffusion model for deconvolution in single molecule localization microscopy.
36 The first stage of our algorithm performs interpolation by computing second order coherence of pixel



37 pairs. Subsequent stages cast localization as a conditional image refinement task, realized by a U-Net
 38 model trained on denoising at various noise levels.

39 This is followed by coordinate refinement by a gradient-based Markov Chain Monte Carlo (MCMC)
 40 scheme, known as Langevin dynamics.

41 2 Background

42 2.1 Degradation Model

43 The central objective of single molecule localization microscopy is to infer a set of molecular
 44 coordinates θ from noisy, low resolution images \mathbf{x} . We define an abstract image stochastic degradation
 45 function F such that $\mathbf{x} = F(\theta)$. In the following paragraphs, we define such a function F .

46 In fluorescence microscopy, each pixel follows Poisson statistics, with expected value

$$\omega = i_0 \int O(u) du \int O(v) dv \quad (1)$$

47 where $i_0 = \eta N_0 \Delta$. The optical impulse response $O(u, v)$ is often approximated as a 2D isotropic
 48 Gaussian with standard deviation σ (Zhang 2007). The parameter η is the photon detection probability
 49 of the sensor and Δ is the exposure time. N_0 represents the number of photons emitted.

50 For a fluorescent emitter located at $\theta = (u_0, v_0)$, we have that

$$\int O(u) du = \frac{1}{2} \left(\operatorname{erf} \left(\frac{u_k + \frac{1}{2} - u_0}{\sqrt{2}\sigma} \right) - \operatorname{erf} \left(\frac{u_k - \frac{1}{2} - u_0}{\sqrt{2}\sigma} \right) \right) \quad (2)$$

51 where we have used the common definition $\operatorname{erf}(z) = \frac{2}{\sqrt{\pi}} \int_0^t e^{-t^2} dt$. For the sake of generality, the
 52 number of photoelectrons at a pixel k , \mathbf{s}_k , is multiplied by a gain factor g_k [ADU/ e^-], which is often
 53 unity. The readout noise per pixel ζ_k can be Gaussian with some pixel-specific offset o_k and variance
 54 σ_k^2 . Ultimately, we have a Poisson component of the signal, which scales with N_0 and may have
 55 Gaussian component, which does not. Therefore, in a single exposure, we measure:

$$\mathbf{x}_t = \mathbf{s}_t + \zeta \quad (3)$$

56 What we are after is the likelihood $p(\mathbf{x}_t|\theta)$ where θ are the molecular coordinates. Fundamental
 57 probability theory states that the distribution of \mathbf{x}_k is the convolution of the distributions of \mathbf{s}_k and ζ_k ,

$$p(\mathbf{x}_t|\theta) = A \sum_{q=0}^{\infty} \frac{1}{q!} e^{-\omega_k} \omega_k^q \frac{1}{\sqrt{2\pi}\sigma_k} e^{-\frac{(\mathbf{x}_k - g_k q - o_k)^2}{2\sigma_k^2}} \quad (4)$$

58 where $P(\zeta_k) = \mathcal{N}(o_k, \sigma_k^2)$ and $P(S_k) = \text{Poisson}(g_k \omega_k)$, A is some normalization constant. In
 59 practice, (4) is difficult to work with, so we look for an approximation. We will use a Poisson-Normal
 60 approximation for simplification. Consider,

$$\zeta_k - o_k + \sigma_k^2 \sim \mathcal{N}(\sigma_k^2, \sigma_k^2) \approx \text{Poisson}(\sigma_k^2) \quad (5)$$

61 Since $\mathbf{x}_k = \mathbf{s}_k + \zeta_k$, we transform $\mathbf{x}'_k = \mathbf{x}_k - o_k + \sigma_k^2$, which is distributed according to

$$\mathbf{x}'_k \sim \text{Poisson}(\omega'_k) \quad (6)$$

62 where $\omega'_k = g_k \omega_k + \sigma_k^2$. This result can be seen from the fact the the convolution of two Poisson
63 distributions is also Poisson. The quality of this approximation will degrade with decreasing signal
64 level, since the Poisson distribution does not retain its Gaussian shape at low expected counts.
65 Nevertheless, the quality of the approximation can be predicted by the Komogonov distance between
66 the convolution distribution (4).

67 3 The Information Bottleneck for Localization

68 Inversion of the degradation function F is generally intractable, particularly when fluorescent
69 molecules are dense within the field of view. This difficulty arises because the parameter θ is
70 typically of large and unknown dimension, rendering maximum likelihood estimation or Markov
71 Chain Monte Carlo sampling computationally difficult. Previous solutions to this problem leverage
72 convolutional neural networks (CNNs) to infer coordinates directly by learning a deterministic im-
73 age transformation F^{-1} , which we refer to as a "localization map" (Nehme 2021). Such methods
74 faithfully capture the information content in degraded images; however, such methods apply arbitrary
75 thresholding to the CNN localization map, potentially creating erroneous localizations, and do not
76 permit sampling.

77 We seek a generative approach, which casts localization as an image restoration problem, where a
78 high resolution kernel density estimate \mathbf{y} is reconstructed from a low resolution image \mathbf{x} . Building
79 on previous efforts, we utilize a CNN learns a representation which compresses \mathbf{x} while preserving
80 the relevant information to the prediction of \mathbf{y} . We use the Fisher information as the information
81 theoretic criteria (Chao 2016). The generative model (6) is also convenient for computing the Fisher
82 information matrix (Smith 2010) and thus the Cramer-Rao lower bound, which bounds the variance
83 of a statistical estimator of θ , from below. The Fisher information is

$$\mathcal{I}_{ij}(\theta) = \mathbb{E} \left(\frac{\partial \ell}{\partial \theta_i} \frac{\partial \ell}{\partial \theta_j} \right) = \sum_k \frac{1}{\omega'_k} \frac{\partial \omega'_k}{\partial \theta_i} \frac{\partial \omega'_k}{\partial \theta_j} \quad (7)$$

84 where the log-likelihood is $\ell(\mathbf{x}_t|\theta)$. We presume a strong model Θ and thus our generative model
85 $P(\mathbf{y}|\mathbf{z}) \approx P(\mathbf{y}|\mathbf{x})$. The CRLB can be used to determine the performance of our model, and thus the
86 quality of the full model (Θ, Φ) .

87 4 Denoising Diffusion Probabilistic Model

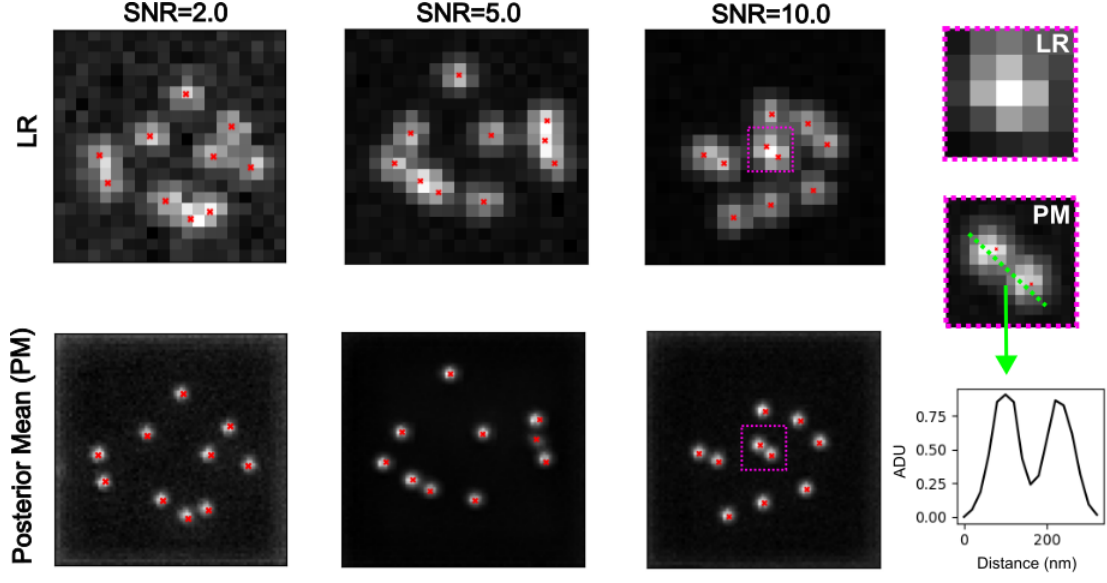
88 Denoising diffusion probabilistic models (DDPM) have emerged as powerful generative models,
89 exceeding GANs and VAEs in a variety of generative modeling tasks. Nevertheless, learning diffusion
90 models directly in data space can limit expressivity of the model (Vahdat 2021). Following this line
91 of work, we build on previous approaches by using a CNN to first compute a localization map, or
92 latent representation $\mathbf{z} = \text{CNN}_{\Theta}(\mathbf{x})$. A denoising diffusion probabilistic model (DDPM) is then used
93 to model the distribution $P_{\Phi}(\mathbf{y}|\mathbf{z})$.

94 Let $\mathbf{y}_0 = \sum_{i=1}^n \omega_n(\sigma)$ be a density estimate of the molecular distribution. The *forward* process is
95 the joint distribution $p_{\theta}(\mathbf{y}_{0:T})$, which is Markovian.

$$q(\mathbf{y}_t|\mathbf{y}_0) = \prod_{t=1}^T q(\mathbf{y}_t|\mathbf{y}_{t-1}) \quad q(\mathbf{y}_t|\mathbf{y}_{t-1}) = \mathcal{N}(\mathbf{y}_{t-1}, \sqrt{\alpha_t} \mathbf{y}_{t-1}, (1 - \alpha_t)I) \quad (8)$$

96 We optimize a denoising model f_{θ} which takes as input an interpolated low-resolution input \mathbf{y} and a
97 noisy input \mathbf{y}_T .

$$p_{\theta}(\mathbf{y}_{0:T}) = p_{\theta}(\mathbf{y}_T) \prod_{t=1}^T p_{\theta}(\mathbf{y}_{t-1}|\mathbf{y}_t) \quad p_{\theta}(\mathbf{y}_{t-1}|\mathbf{y}_t) = \mathcal{N}(\mathbf{y}_{t-1}, \mu_{\theta}(\mathbf{y}_t, \gamma_t), \sigma_t^2 I) \quad (9)$$



where $\gamma_t = \prod_{i=1}^t \alpha_t$. Note that the model θ is not a function of t . The mean of the transition density reads

$$\mu_{\theta}(\mathbf{x}_t, \mathbf{y}, \gamma_t) = \frac{1}{\sqrt{\alpha_t}} \left(\mathbf{y}_t - \frac{1 - \alpha_t}{\sqrt{1 - \gamma_t}} f_{\theta}(\mathbf{x}_t, \gamma_t) \right) \quad (10)$$

5 Experiments